4: Engineered Square Patch Dielectric Absorbers

An implementable design approach to extend the bandwidth of existing Dielectric Material Based Microwave Absorbers (DMBMA) is investigated. The design comprises of planar square patches of DMBMA placed periodically on the metal-backed FR4 sheet. For demonstration purpose, the DMBMA is synthesized by adding conducting carbon fillers in the polyurethane matrix, and its electromagnetic parameters are measured in X-band. A single reflection minima is observed in DMBMA owing to $\lambda/4$ resonance. In comparison, the bandwidth of 8 GHz (10-18 GHz) is achieved for –10 dB reflection for square patch-based DMBMA. An additional resonant mode is observed due to capacitive coupling between the square patches. The enhanced bandwidth is attributed to the overlapping of $\lambda/4$ resonance and induced coupling mode. A good agreement between the simulated and measured data is observed.

4.1 DESIGN AND RESULTS

4.1.1 Synthesis of Dielectric Absorber

The purpose of synthesizing DMBMA is to support the proposed design approach. The detailed discussion regarding the design, analysis and physical realization of desired material parameters are reported in [Qin and Brosseau, 2012], [Rozanov, 2000], [Brosseau *et al.*, 2001], [Tuncer *et al.*, 2001], [Cheng *et al.*, 2012] and [Koledintseva *et al.*, 2006]. The interaction of EM waves with the material is characterized by its constitutive parameters viz. permittivity and permeability. The EM material's real and imaginary parameters are related by *Kramers–Kronig* relations [Rozanov, 2000]. Owing to its dependence, arbitrary values cannot be considered. The permeability of the material cannot be tuned as per the desired level due to Snoek's limit [Rozanov, 2000]. The dielectric absorbers provide flexibility in terms of less weight penalty and ease of synthesis process. The dielectric absorbers are characterized by its real and imaginary parts of permittivity due to the non-magnetic response. The dielectric absorber is synthesized by adding 6% w/w conducting carbon in a polyurethane matrix. Homogenous dispersion of the filler in the polyurethane matrix is carried out using a ball milling process, a widely used technique in material synthesis [Suryanarayana, 2001]. The material parameters of the control sample (polyurethane resin) and composite (carbon filler in the polyurethane matrix) are measured in X-band using waveguide method. The measured permittivity and permeability of the synthesized composite are shown in Figure 4- 1. It is noted that by adding conducting filler in a polyurethane matrix, the material parameters can be tuned. Owing to the dielectric nature of the filler, the permittivity values of the composite change significantly whereas the permeability values remain almost invariant.

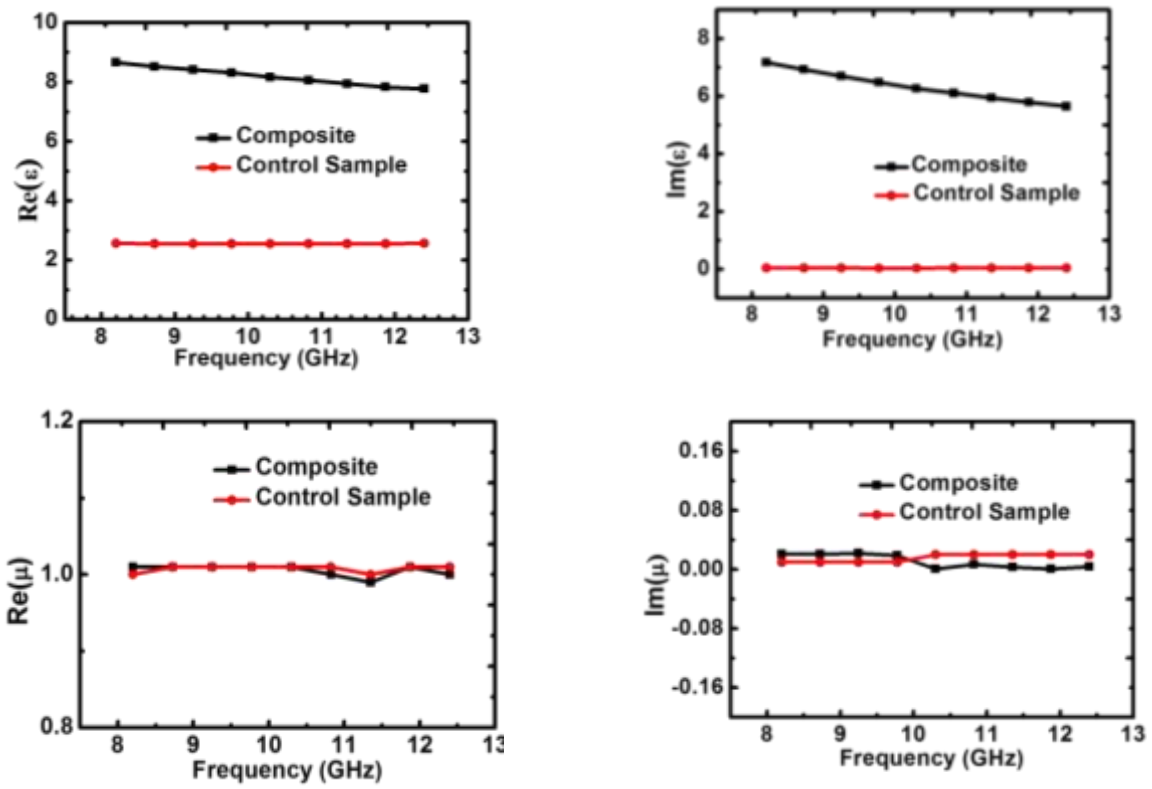

Figure 4- 1: Measured the real and imaginary part of the material parameters of the control sample and composite

The S-parameters of designed absorbers are simulated in CST Microwave Studio using frequency-domain solver under unit cell boundary conditions. The material parameters as presented in Figure 4- 1 are plugged in the dispersive material list of CST Microwave Studio and mathematically fitted with 2nd order polynomial. The absorbance of the metal-backed absorber is calculated using the relation $A(\omega) = 1 - R(\omega) = 1 - |S_{11}|^2$. By minimizing the reflectance, the absorbance can be enhanced. The performance of the absorber is simulated for different polarization angles and oblique incidence for TE and TM components.

4.1.2 Design of Dielectric Absorber

The impedance and return loss of material based absorber are expressed as [Qin and Brosseau, 2012]:-

$$Z_d = Z_0\sqrt{\frac{\mu}{\varepsilon}}\tanh\left(\frac{-j2\pi f d\sqrt{\mu\varepsilon}}{c}\right) \quad (1)$$

$$RL\ (dB) = 20\ log_{10}\left|\frac{Z_d - Z_0}{Z_d + Z_0}\right| \quad (2)$$

where $Z_d, Z_0, f, d, \varepsilon, \mu$ and c are the material impedance, free space impedance, frequency, thickness, permittivity, permeability and speed of light respectively. The material impedance can be tailored by permittivity, permeability and thickness. For quarter wavelength thickness, the absorber forms an open transmission line which results in reflection minima because of impedance matching condition [Watts *et al.*, 2012].

The unit cell of the DMBMA is comprised of a layered arrangement of, bottom to the top, metal sheet, FR4 sheet and synthesized composite, as shown in Figure 4-2(a). The utility of FR4 spacer is discussed in Section-4.4. The permittivity and dielectric loss tangent of FR4 are 4.2 and

0.02, respectively. The thickness of the FR4 sheet and dielectric absorber are referred to as tfr =1 mm and d =1.75 mm, respectively.

The simulated return loss of synthesized absorber is depicted in Figure 4-2(b) for different values of d and tfr=1 mm. For the dielectric absorber, a single-mode is observed due to λ/4 resonance (where λ is the wavelength in the medium) [Wang *et al.*, 2011][14]. The resonant peak shifts towards lower frequency region as the dielectric absorber's thickness increases.

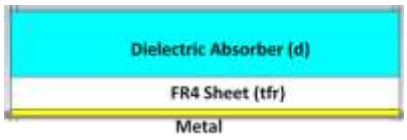

(a)

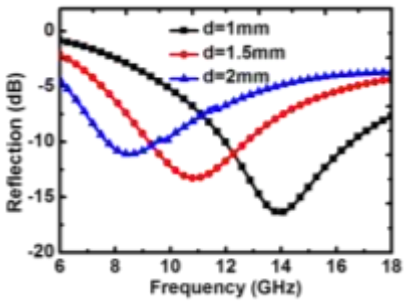

(b)

Figure 4-2: Side view of the unit cell of the dielectric absorber (b) Simulated reflection of synthesized dielectric absorber for different d values and tfr=1mm

4.1.3 Design of Square Patch DMBMA

The side and top view of unit cell of the Square Patch DMBMA are shown in Figure 4-3(a) and (b) respectively. The unit cell of the absorber consists of, bottom to top, a metal sheet, FR4 spacer and square patches of DMBMA. The design parameters are p (unit cell dimension) = 12 mm, a (square patch dimension) = 10mm, tfr (FR4 thickness) = 1 mm and d (dielectric absorber thickness) = 1.75 mm.

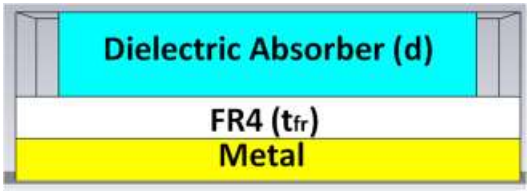

(a)

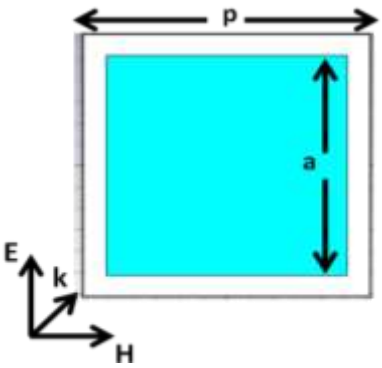

(b)

Figure 4-3: (a) & (b) Side and top view respectively, of the unit cell of the absorber along with wave vector, electric and magnetic field for p=12mm, a=10mm, d=1.75 mm and tfr=1mm

Figure 4-4(a) shows the orientation of wave vector, electric field and magnetic field for different polarization angle. The wave vector is always along the z-direction whereas the electric and magnetic fields are changed by an angle Φ simultaneously with respect to y and x-directions respectively. The performance of the absorber is almost invariant due to four-fold rotational symmetry as shown in Figure 4-4(b) [[Zhu *et al.*, 2010], [Lu *et al.*, 2012].

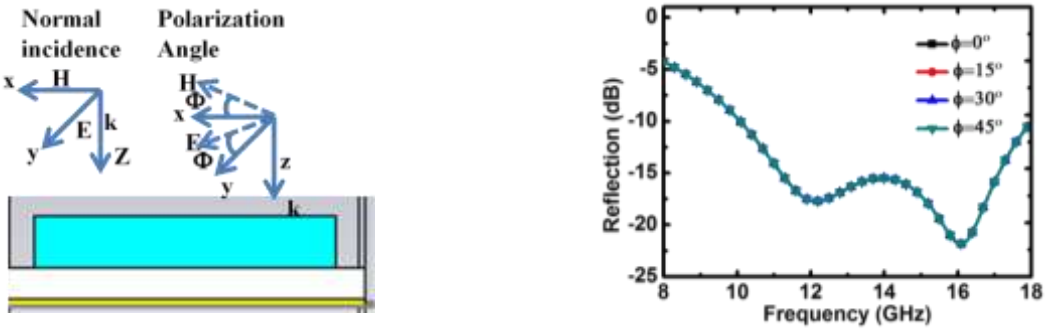

(a) (b)

Figure 4-4: (a) Orientation of the wave vector, electric field and magnetic field for different polarization angles (b) Simulated results for polarization angles 0° to 45°

It is noted that for frequency region 10 GHz to 18 GHz, the reflection is below –10 dB with a bandwidth of 8 GHz (Figure 4-4(b)). The two reflection minimas are observed at 12 GHz and 16 GHz. The parametric analysis of geometric parameters indicates the minima at 12 GHz mainly arises from λ/4 resonance, whereas the minima at 16 GHz originates due to the coupling between the square patches. Figure 4-5(a)and (c) presents the orientation of the wave vector, electric field and magnetic field for oblique incidence under TM and TE modes respectively. In TM/TE mode, magnetic field/electric field is aligned in x/y direction whereas the wave vector and electric field/ magnetic field are changed simultaneously by an angle θ with respect to z and y/x direction respectively [Bhattacharyya, 2016]. The results for oblique incidence 0° to 60° under TM and TE modes are plotted in Figure 4-5(b) and (d) respectively. The performance of the absorber for -10 dB reflection is almost stable up to 30° for oblique incidence under TE and TM mode, respectively.

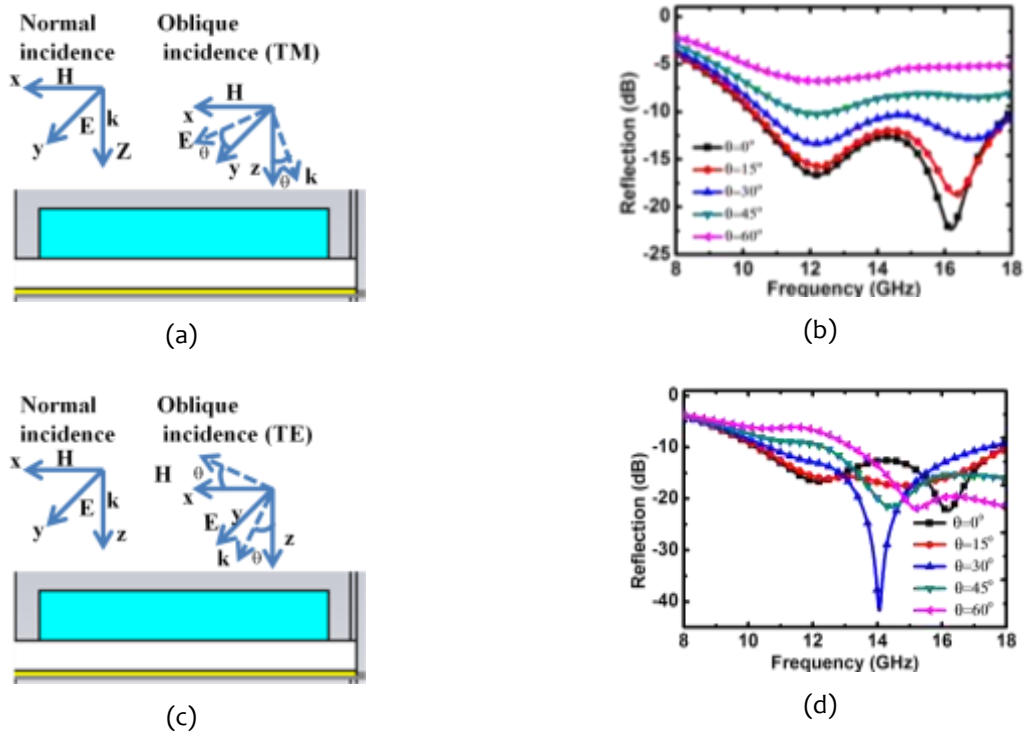

(a) (b)

(c) (d)

Figure 4-5: (a) and (c) Orientation of the wave vector, electric field and magnetic field for oblique incidence under TM and TE modes respectively (b) and (d) Simulated results for oblique incidence 0° to 60° under TM and TE modes respectively

4.2 ANALYSIS AND DISCUSSION

4.2.1 Effect of Square Patch Size

The simulated reflection for different square patch size is plotted in Figure 4-6. It is evident that for a=12mm=p, the single resonant mode is observed at 9 GHz due to λ/4 resonance. For a=11mm, two reflection minimas are noted at 11 GHz and 15 GHz. The decrease in patch size shifts the reflection dip to the higher frequency region. It is also noted that the minimas are well separated as the patch size decreases. For a=10 mm, the minimas are well overlapped and result in 8 GHz bandwidth for -10 dB reflection (Figure 4-4(b)).

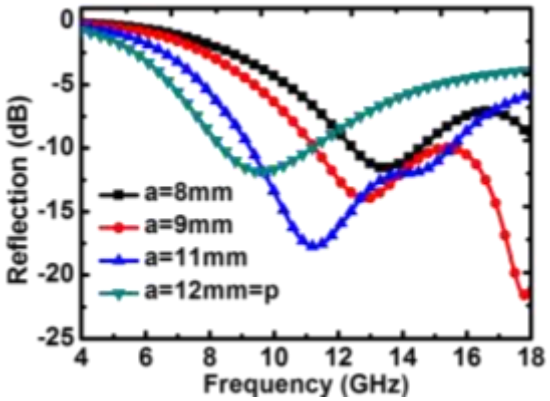

Figure 4-6: Simulated reflection for different square patch sizes (d=1.75 mm and tfr=1mm)

The origin of the additional minima is attributed to the formation of capacitance between the edges of square patches [Luukkonen *et al.*, 2009]. The strength of the coupling is dependent on the size and spacing of the square patch for the given dielectric material [Luukkonen *et al.*, 2009]. As the spacing between the patches is decreased, the coupling minima shifts to lower frequency due to the increased coupling strength. The increase in spacing leads the coupling minima shifts towards higher frequency due to the decrease in coupling strength. For a=p=12mm, the capacitance due to square patch vanishes and results in single resonance dip as observed in DMBMA. It is noted that as the square patch size decreases the λ/4 resonance shifts to a higher frequency. The square patches decrease the material impedance, which shifts the absorbance peak to a higher frequency [Costa *et al.*, 2010].

4.2.2 Physical Insight

The field quantities are numerically estimated to support the claim regarding the origin of the additional absorbing peak. The field quantities are estimated for d=1.75mm, p=12mm, a=10mm and tfr=1mm at absorbing frequencies 12 GHz and 16 GHz (Figure 4-7).

In case of 12 GHz, the electric field is confined in the middle of dielectric absorber due to dielectric nature (Figure 4-7(a)), leading to maximum power loss density in the middle of the dielectric absorber. In contrast, the electric field is concentrated at the edges of the square patches at 16 GHz. The large electric field indicates the presence of electrical charges (Figure 4-7(b)). The large electric field at the edges leads to the presence of the capacitive feature. At 12 GHz, the power loss density is maximum in the middle of the dielectric absorber. (Figure 4-7(c)) This loss distribution indicates that the energy is dissipated as dielectric losses. On the other hand, the power loss density is concentrated at the edges of the square patches at 16 GHz. The electric field and loss distribution at 16 GHz (Figure 4-7(b) and (d)) support the claim regarding the capacitive coupling between the square patches.

`

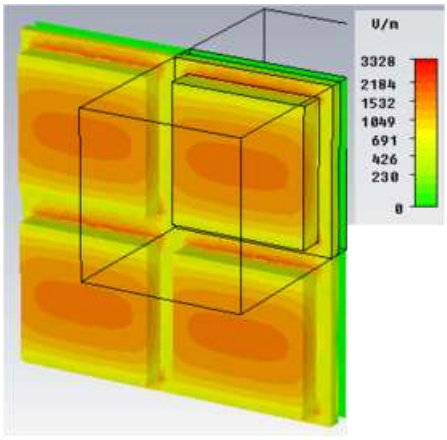

(a) Electric Field 12 GHz

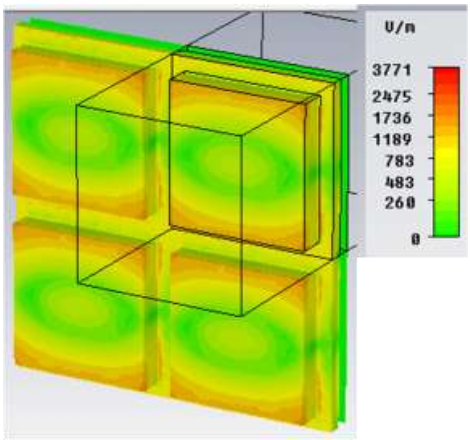

(b) Electric Field 16 GHz

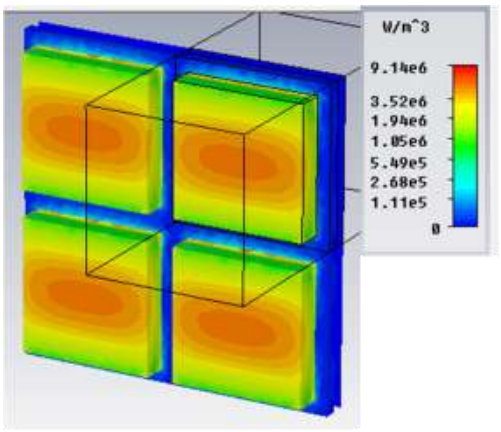

(c) Power loss 12 GHz

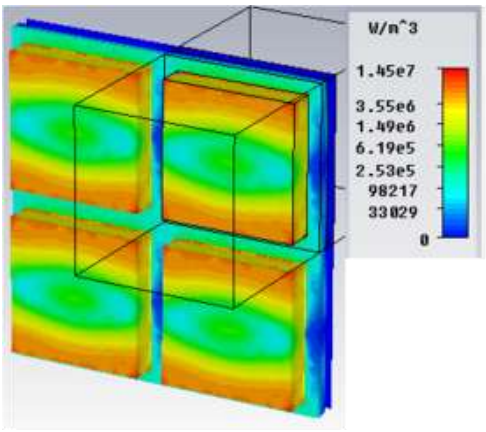

(d) Power loss 16 GHz

Figure 4-7: Simulated electric field and power loss distribution at absorbing frequencies 12 GHz and 16 GHz respectively

4.3 FABRICATION AND EXPERIMENTAL RESULTS

4.3.1 Dielectric Absorber

The synthesized DMBMA is shown in Figure 4-8(a) with dimensions 115 mm x 115 mm x 2.75 mm. The $\lambda/4$ resonance absorption peak of the synthesized dielectric absorber is at approximately 16.1 GHz for d=1.75 mm. The FR4 spacer is used to increase the thickness of the synthesized absorber to measure the reflection in 3-18 GHz range. The mismatch between the simulation and the measurement results can be attributed to the thickness variation of the synthesized DBMA, and the mathematical fitting used in Sec. 4.1.1 for the constitutive parameters. The representative measurement setup is depicted in Figure 4-8(b). The reflection measurement of designed absorbers is carried out in an anechoic chamber using Vector Network Analyzer (VNA) and a pair of horn antennas as described in [Cheng and Yang, 2010] and [Li, *et al*, 2010]. The experimental and simulated reflection of the synthesized absorber is shown in Figure 4-8(c). The deviation in the results is attributed to fabrication and experimental errors.

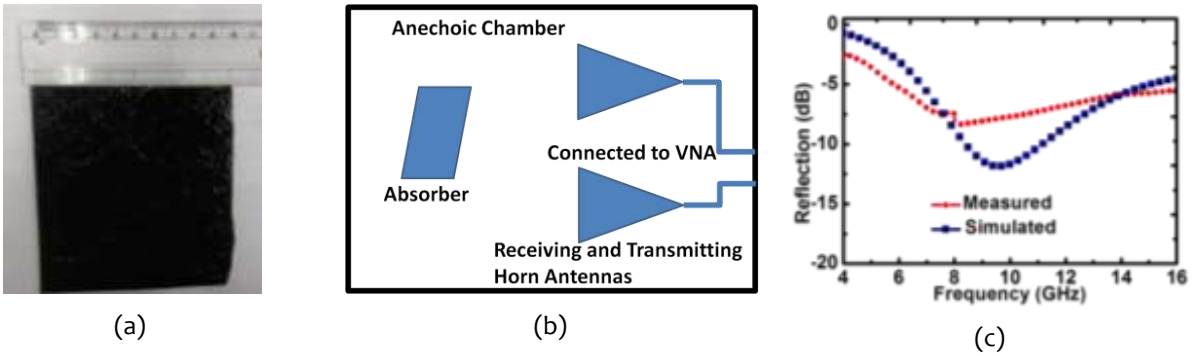

(a) (b) (c)

Figure 4-8: (a) Synthesized dielectric absorber (b) Schematic of measurement setup (c) Simulated and measured reflection of the dielectric absorber

4.3.2 Square Patch Dielectric Absorbers

The designed absorber is physically realized by cutting the square patches of the synthesized dielectric absorber of dimensions 10 mm x 10 mm. These square patches are placed manually, on metal-backed FR4 sheet with a periodicity of 12 mm using an epoxy-based adhesive. The fabricated absorber, having the dimensions 120 mm x 120 mm x 2.75 mm, is shown in Figure 4-9(a). The simulated and measured results are shown in Figure 4-9(b).

A good agreement between the measured and simulated results validates the design of the absorber. The slight deviation is attributed to the variation of spacing between the square patches due to manual alignment (Figure 4-9(a)). The experimental results indicate the bandwidth of 8 GHz for -10 dB reflection.

The reflection from the absorber is measured for varying aspect angles at different frequencies and compared with the metal sheet. The aspect angle is the angular orientation of the absorber with respect to the antennas where the positions of the antennas are remained fixed [Brumley, 1988].

The reflection from the absorber is less in comparison to the metal, as shown in Figure 4-9((c) to (f)). For the given aspect angle, the difference between the metal and absorber reflection gives the absorbance of the absorber. The performance of the absorber is stable for the small aspect angle. The low angular stability is attributed to small permittivity values of the synthesized DMBMA [Costa *et al.*, 2013], [Chambers, 1994]. The angular stability of the absorber can be improved by increasing the real part of permittivity.

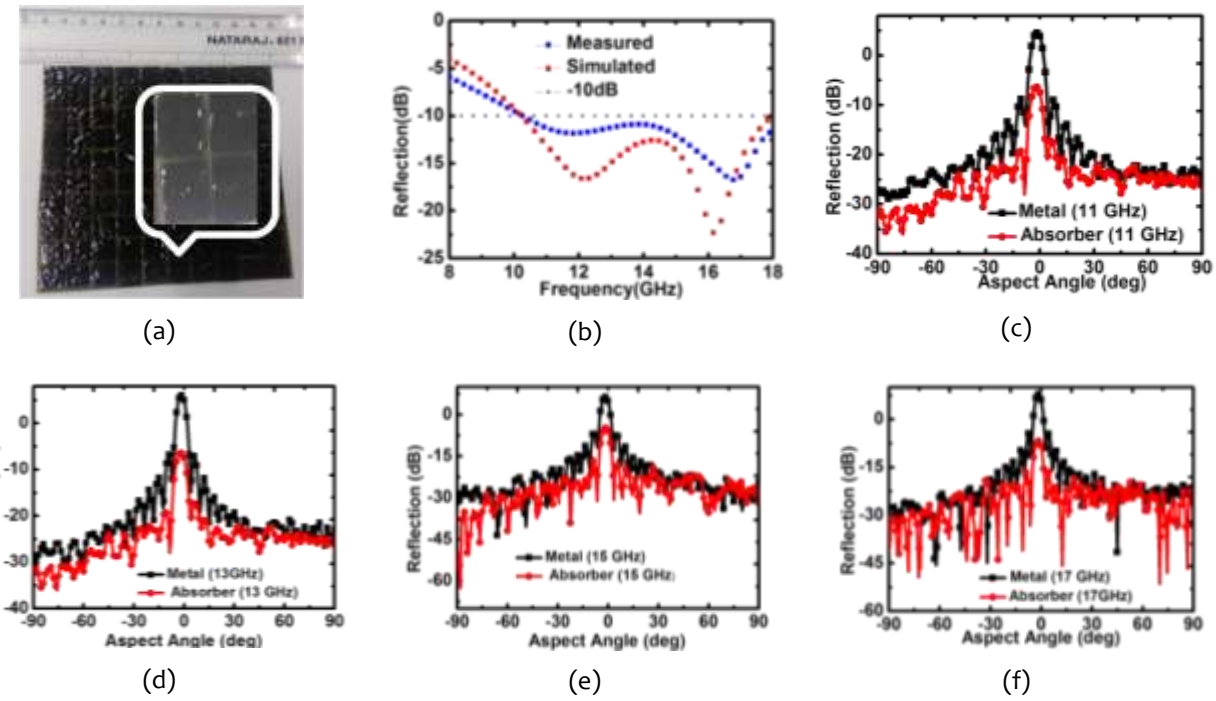

(a) (b) (c)

(d) (e) (f)

Figure 4-9: (a) Fabricated square patch based dielectric absorber (b) Simulated and experimental results for square patch based dielectric absorber ((c) to (f)) Measured reflection from metal and absorber for varied aspect angle at different frequencies

In summary, the chapter suggests the simple and implementable design approach to improve the bandwidth of available DMBMA. The bandwidth improvement is attributed to simultaneously overlapping of $\lambda/4$ mode and an additional induced mode due to capacitive coupling between the square patches of DMBMA. The bandwidth of DMBMA can be further improved by designing the unit cell consisting of square patches of different DMBMA with varied thickness. The designed absorber finds a wide range of applications in civil, commercial and defence sectors. For practical applications, these absorbers should qualify standard mechanical and environmental test parameters.